Int. J. Heat Mass Transfer. Vol. 30, No. 2, pp. 401–405, 1987
Printed in Great Britain

0017-9310/87 $3.00+0.00
Pergamon Journals Ltd.

Thermodynamic optimization of convective heat transfer through a duct with constant wall temperature

P. K. NAG* and P. MUKHERJEE

Department of Mechanical Engineering, Indian Institute of Technology, Kharagpur 721302, India

(Received 29 April 1985 and in final form 6 May 1986)

1. INTRODUCTION

MOST convective heat transfer processes are characterized by two types of losses, namely: losses due to fluid friction and those due to heat transfer across a finite temperature difference. However, these two interrelated phenomena are both manifestations of thermodynamic irreversibility and the investigation of a process from this single standpoint is known as the second law analysis. There exists a direct proportionality between irreversibility, quantified in the entropy generated, and the amount of useful and available work lost in the process. Second law analysis seeks to minimize this loss by keeping the entropy generated to the minimum.

Bejan [1–5] has analysed heat transfer from ducts with constant heat flux for flat plates, cylinders in cross flow and rectangular ducts, and has designed counterflow heat exchangers for gas-to-gas applications and supports for cryogenic apparatus. Sarangi and Chowdhury [6] have analysed counterflow heat exchangers, accounting for the entropy generated due to axial conduction in addition to lateral heat transfer and fluid friction, and have found an optimum thermal conductivity of the wall. Golem and Brzustowski [7] examined the irreversibility of heat exchangers using Reistad effectiveness which in the limiting case of a reversible heat exchanger becomes equal to unity. In connection with the maximum available work which could be harvested from solar radiation, Parrot [8] found an expression for solar energy which was used by him and Kreider [9] for determining the efficiency of solar power installations. London [10] has presented an operationally convenient methodology for pricing the penalties of thermodynamic irreversibilities.

However, the important case of heat transfer from a duct with constant wall temperature, as happens when there is a phase change on one side of a heat exchanger tube, has not been investigated and we now attempt to do this. The entropy generation rate expressed nondimensionally when plotted against the nondimensional initial temperature difference, τ, shows a distinct minimum, and this optimum value of τ is then plotted against J, a duty parameter representing heat transfer, for various values of n, the length-to-radius ratio of the duct. Next it is shown that the conventional wisdom of seeking to maximize the ratio of heat transfer to pumping power, R, is not consistent with the second law analysis. The entropy generation rate is plotted against R for various values of J and these curves too show clear minima implying that an optimum exists. This optimum value of R yields an optimum fluid velocity and is also plotted against J for various values of n.

2. ENTROPY GENERATION

By energy balance of the control volume of length dx of the duct with constant wall temperature T_w (Fig. 1)

$$h_c 2\pi r\,dx\,\theta = -\pi r^2 U\rho c_p\,d\theta. \quad (1)$$

On integration

$$\theta = \theta_0 \exp(-Ax/r) \quad (2)$$

and θ_0 is the initial temperature difference and A is equal to twice the Stanton number.

Considering an entropy balance in the same control volume, the rate of entropy generation is

$$d\dot{S}_{gen} = \dot{m}\,ds - \frac{dQ}{T_w}. \quad (3)$$

Assuming the fluid to be an ideal gas or to be incompressible, $dh = c_p\,dT$, and using the thermodynamic relation $T\,ds = dh - v\,dp$, and $dQ = \dot{m}\,dh$, equation (3) can be written as

$$\frac{d\dot{S}_{gen}}{dx} = -\dot{m}c_p\frac{T-T_w}{TT_w}\frac{dT}{dx} + \frac{\dot{m}}{\rho T}\left(-\frac{dP}{dx}\right). \quad (4)$$

Substituting the values of $T-T_w$, T and dT/dx from equation (2)

$$\frac{d\dot{S}_{gen}}{dx} = \frac{\dot{m}c_p A}{r}\frac{[\tau\exp(-Ax/r)]^2}{[1+\tau\exp(-Ax/r)]} + \frac{\dot{m}}{\rho T_w}\left(-\frac{dP}{dx}\right)\frac{1}{[1+\tau\exp(-Ax/r)]} \quad (5)$$

where τ is the non-dimensional initial temperature difference. On integration along the length of the duct

$$\dot{S}_{gen} = \dot{m}c_p\{\tau[1-\exp(-An)] + \ln[(1+\tau\exp(-An))/(1+\tau)]\} + \frac{\dot{m}r(-dP/dx)}{\rho T_w A}\cdot\ln\frac{1+\tau\exp(-An)}{(1+\tau)\exp(-An)}. \quad (6)$$

Defining the entropy generation unit N_s as

$$N_s = \frac{\dot{S}_{gen}}{\dot{m}c_p} \quad (7)$$

and substituting

$$-\frac{dP}{dx} = \frac{f\rho U^2}{r} \quad (8)$$

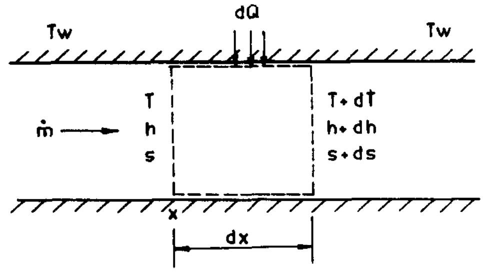

FIG. 1.

* Present address: Centre for Energy Studies, Technical University of Nova Scotia, P.O. Box 1000, Halifax, Canada B3J 2X4.

NOMENCLATURE

a	cross-sectional area of duct
A	$2St$
c_p	specific heat at constant pressure
f	friction factor
h	specific enthalpy
h_c	average heat transfer coefficient
J	non-dimensional duty parameter defined in equation (11)
k	thermal conductivity of fluid
L	length of duct
$\dot{m}$	mass flow rate
M	non-dimensional parameter defined in equation (18)
n	L/r ratio of duct
N_s	non-dimensional entropy generation number defined in equation (7)
N	non-dimensional parameter defined in equation (14)
P	pressure
Q	total heat transfer rate from duct
r	radius of duct
R	ratio of heat transfer rate to pumping power
s	specific entropy of fluid
$\dot{S}_{gen}$	rate of entropy generation
St	Stanton number, $h_c/(\rho c_p U)$
T	fluid temperature
T_0	initial fluid temperature
T_w	constant wall temperature
U	mean fluid velocity
v	specific volume of fluid
x	axial distance along the duct.

Greek symbols

θ	temperature difference between fluid and wall, $T-T_w$
θ_0	initial temperature difference between fluid and wall, T_0-T_w
ρ	fluid density
τ	non-dimensional initial temperature difference, θ_0/T_w.

and

$$U = \frac{Q}{\theta_0 a c_p \rho[1-\exp(-An)]}. \qquad (9)$$

(by re-arrangement)

Equation (6) can be written as

$$N_s = \tau[1-\exp(-An)]+\ln\{[1+\tau\exp(-An)]/(1+\tau)\} + \frac{J^2}{\tau^2 A[1-\exp(-An)]^2}\cdot\ln\frac{1+\tau\exp(-An)}{(1+\tau)\exp(-An)} \qquad (10)$$

where J is the duty parameter defined as

$$J = \frac{f^{1/2}Q}{\rho a(c_p T_w)^{3/2}} \qquad (11)$$

which accounts for the required heat transfer rate, fluid properties, wall temperature and duct cross-section.

Numerical evaluation of equation (10) is done with air as the fluid and a Stanton number as 0.005 [11]. Figure 2 shows the variation of N_s with τ for $n = 60$, $A = 0.01$ and J as a parameter, while Fig. 3 shows the variation of N_s with τ for $J = 2\times10^{-5}$, $A = 0.01$ and n as a parameter. In Fig. 2 the entropy generation number N_s has been normalized with respect to J to facilitate drawing of the curves, as otherwise the three curves would be widely separated on the X–Y plane. In Fig. 3 though no such normalization was called for, it has been done to facilitate comparison with Fig. 2. These two sets of curves show that N_s is a strong function of τ and also passes through a minimum value as τ is increased from zero. This minimum point is the optimum which the second law analysis seeks.

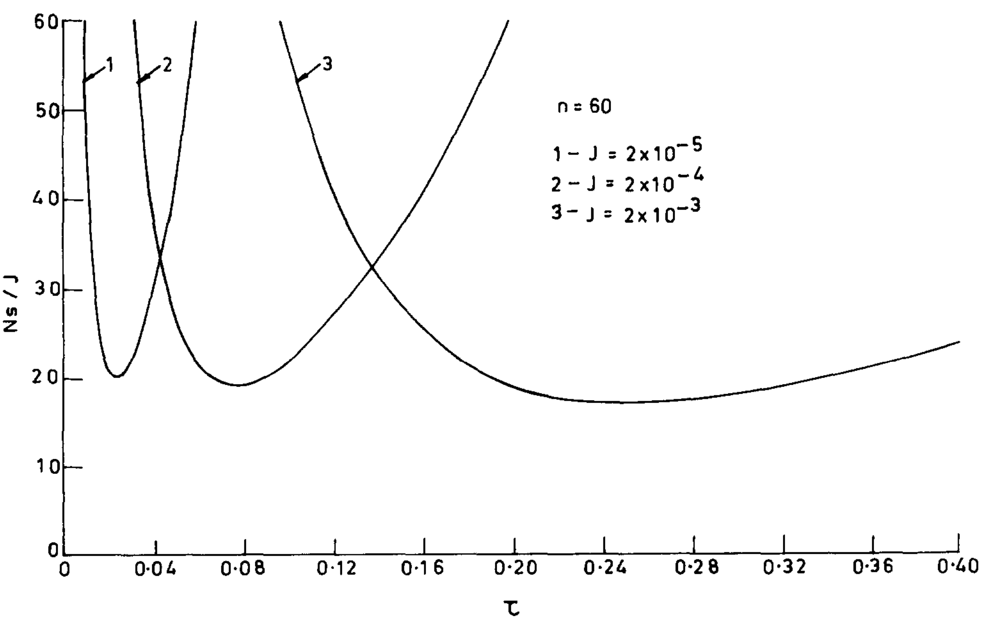

FIG. 2.

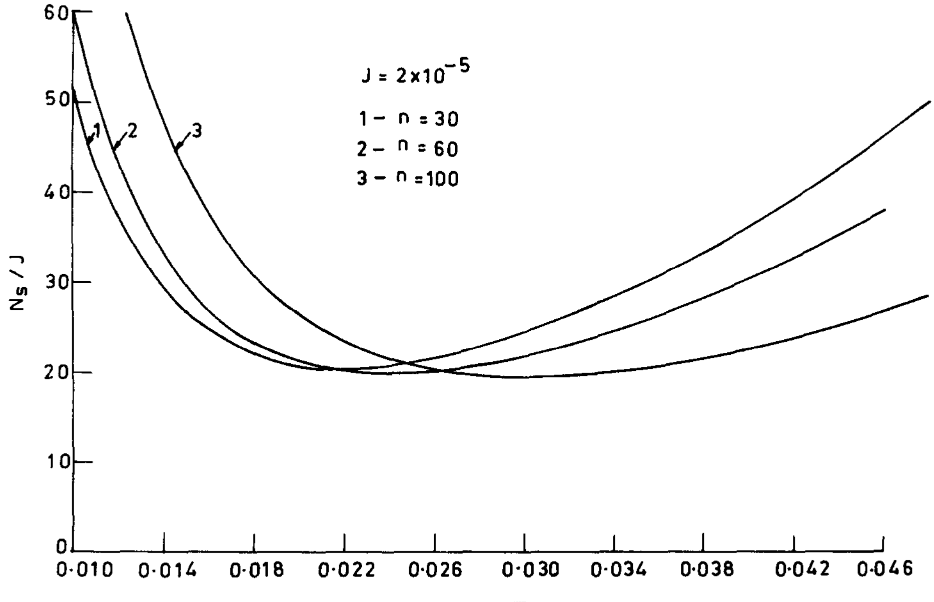

FIG. 3.

3. OPTIMUM VALUES

3.1. *Optimum* τ

For $\tau \ll 1$, equation (10) can be written as

$$N_s = \tau[1-\exp(-An)]+\ln\frac{1+\tau\exp(-An)}{1+\tau} + \frac{J^2 n}{\tau^2[1-\exp(-An)]^2}. \quad (12)$$

By differentiating N_s with respect to τ and equating it to zero, the optimum value of τ is obtained as

$$\tau_{opt} = \frac{\sqrt{J}}{N} \quad (13)$$

where

$$N = \left[\frac{[1-\exp(-2An)][1-\exp(-An)]^2}{2n}\right]^{1/4}. \quad (14)$$

The values of τ_{opt} have been plotted against J in Fig. 4 for air with $A = 0.01$ and with n as a parameter. It shows that for a particular heat load, there is an optimum initial tem-

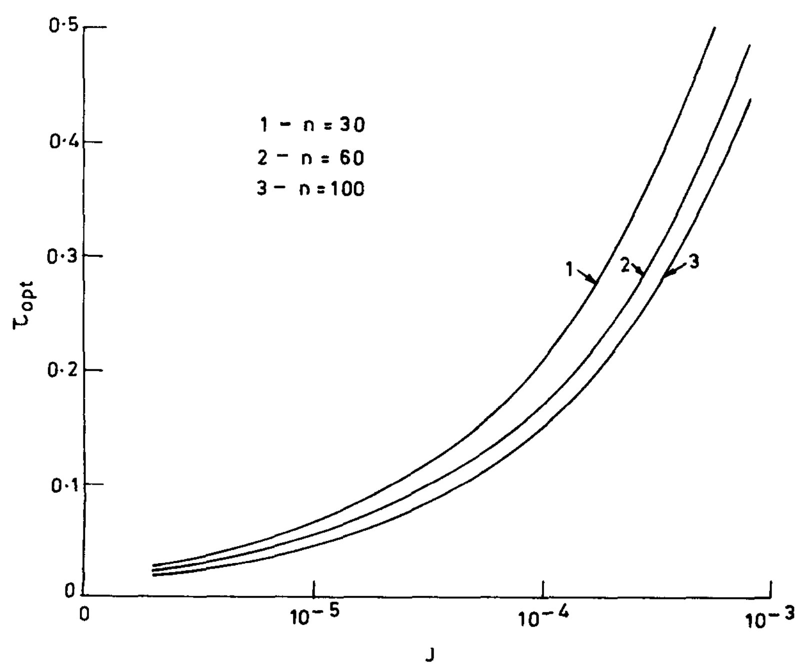

FIG. 4.

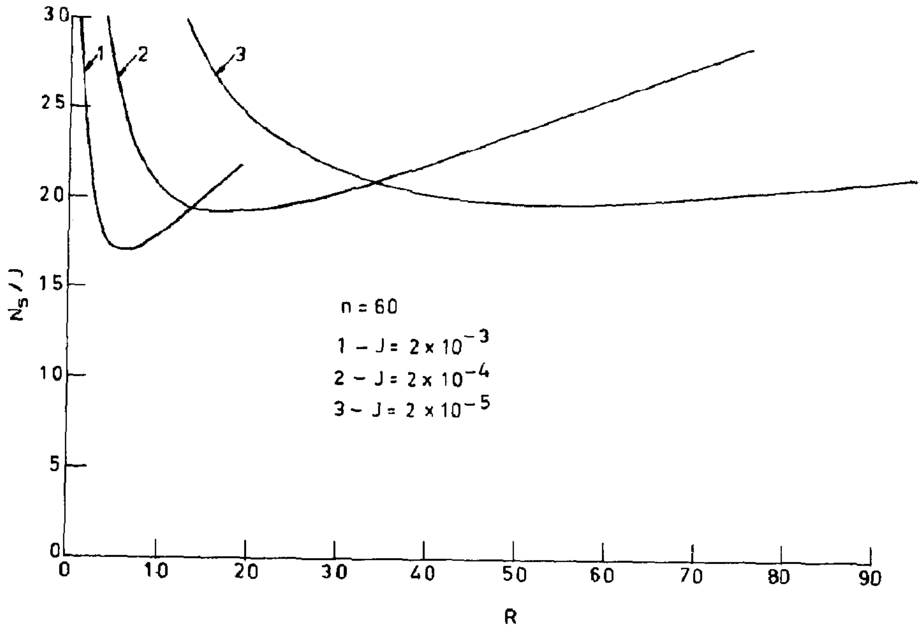

FIG. 5.

perature difference between the fluid and the wall which corresponds to the minimum irreversibility.

3.2. *Optimum R*

Defining the ratio of heat transfer to pumping power R as

$$R = \frac{Q}{a\Delta PU} \tag{15}$$

and substituting equations (8) and (9)

$$R = \frac{\tau^3[1-\exp(-An)]^3}{J^2 n}. \tag{16}$$

Since R is a function of τ and N_s is also a function of τ, hence N_s is functionally dependent on R. This dependence is shown in Fig. 5 for air with $A = 0.01$, $n = 60$ and J as a parameter. Again, a distinct minimum of N_s is visible in each of the curves. Since τ_{opt} corresponds to the minimum value of N_s, the substitution of τ_{opt} from equation (13) in (16) yields R_{opt} as given below

$$R_{opt} = \frac{M}{\sqrt{J}} \tag{17}$$

where

$$M = \left[\frac{2[1-\exp(-An)]^6}{n[1-\exp(-2An)]^3}\right]^{1/4}. \tag{18}$$

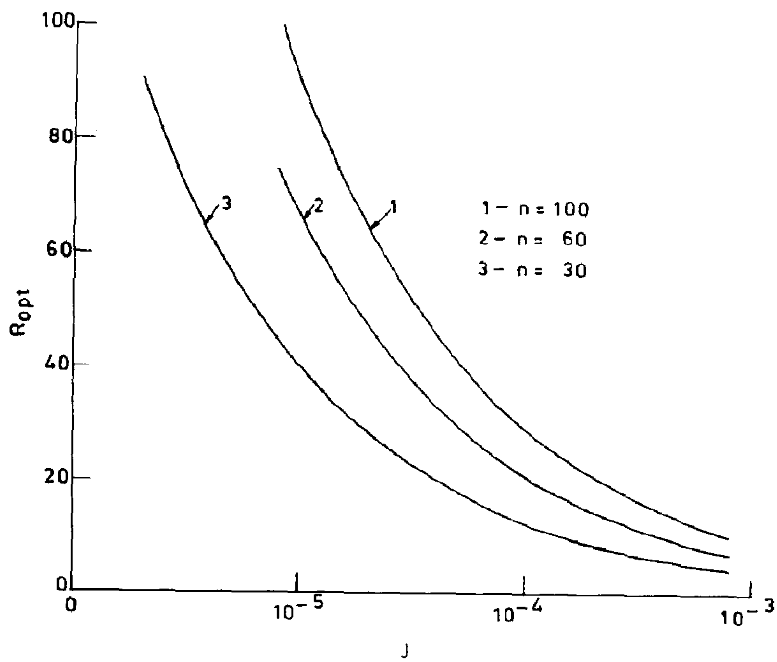

FIG. 6.

The variation of R_{opt} with J is shown in Fig. 6 with $A = 0.01$ and n as a parameter. For a particular value of J (i.e. heat load), there is an optimum value of R which should be used. In other words, using

$$\Delta P = \frac{f\rho U^2 L}{r} \tag{19}$$

in equation (15)

$$U_{opt} = \left[\frac{Q}{\pi r f \rho L R_{opt}}\right]^{1/3}. \tag{20}$$

Thus there is an optimum fluid velocity which corresponds to the minimum loss of available power and should be recommended in the design of the heat exchanger.

4. CONCLUSIONS

This analysis shows that in any heat transfer application with the constant wall temperature boundary condition, the initial temperature difference between the fluid and the wall is an important design criterion and should be set at the optimum value. There is an optimum ratio of the heat transfer to pumping power which should be used. Simply maximizing this ratio is not often a good solution, since in that case the entropy generated may be far from the minimum possible and a large amount of the available energy may thus be irretrievably lost. An optimum fluid velocity corresponding to the minimum irreversibility is recommended for the design of such a heat exchanger.

REFERENCES

1. A. Bejan, General criterion for rating heat exchanger performance, *Int. J. Heat Mass Transfer* **21**, 665 (1978).
2. A. Bejan, A study of entropy generation in fundamental convective heat transfer, *J. Heat Transfer* **101**, 718 (1979).
3. A. Bejan, The concept of irreversibility in heat exchanger design: counterflow heat exchanger for gas-to-gas applications, *J. Heat Transfer* **99**, 374 (1977).
4. A. Bejan and A. L. Smith, Thermodynamic optimization of mechanical supports for cryogenic apparatus, *Cryogenics* **14**, 158 (1974).
5. A. Bejan and A. L. Smith, Heat exchangers for vapour cooled conducting supports of cryostats, *Adv. Cryogenic Engng* **21**, 247 (1975).
6. S. Sarangi and K. Chowdhury, On the generation of entropy in counterflow heat exchangers, *Cryogenics* **22**, 63 (1982).
7. P. J. Golem and T. A. Brzustowski, Second law analysis of thermal processes, *Trans. CSME* **4**, 219 (1977).
8. J. E. Parrot, Theoretical upper limit to the conversion efficiency of solar energy, *Sol. Energy* **21**, 227 (1978).
9. J. F. Kreider, Second law analysis of solar thermal processes, *Energy Res.* **3**, 325 (1979).
10. A. L. London, Economics and the second law, *Int. J. Heat Mass Transfer* **25**, 743 (1982).
11. E. R. G. Eckert and R. M. Drake, *Analysis of Heat and Mass Transfer*, p. 373. McGraw-Hill Kogakusha, Tokyo (1972).

Int. J. Heat Mass Transfer. Vol. 30, No. 2, pp. 405–408, 1987
Printed in Great Britain

0017-9310/87 \$3.00+0.00
Pergamon Journals Ltd.

Correlations for laminar mixed convection on vertical, inclined and horizontal flat plates with uniform surface heat flux

B. F. ARMALY, T. S. CHEN and N. RAMACHANDRAN

Department of Mechanical and Aerospace Engineering, University of Missouri–Rolla, Rolla, MO 65401, U.S.A.

(*Received* 4 *November* 1985 *and in final form* 26 *June* 1986)

INTRODUCTION

MIXED convection accounts for the buoyancy effects on forced flows or the forced flow effects on buoyant flows. Published results on mixed convection flows do not cover the entire mixed convection regime and, in addition, the uniform wall temperature case (UWT) has received significantly more attention than the uniform wall heat flux case (UHF). A relatively comprehensive summary on mixed convection in external flows has been given recently by Chen *et al.* [1].

To summarize the analytical studies for mixed convection adjacent to flat plates under the UHF heating condition, it is noted that the local Nusselt number results have been presented for vertical plates covering $0 \leqslant Gr_x^*/Re_x^{5/2} \leqslant 2.8$ for $0.1 \leqslant Pr \leqslant 100$ [2], inclined plates covering $-0.25 \leqslant Gr_x^* \cos\gamma/Re_x^{5/2} \leqslant 5$ for $Pr = 0.7$ and 7 [3] and $-1 \leqslant Gr_x^*/Re_x^{5/2} \leqslant 2$ for $Pr = 0.7$ and 7 [4], and horizontal plates covering $0 \leqslant Gr_x^*/Re_x^3 \leqslant 1$ for $Pr = 0.7$ [5]. Thus, it is clear that the heat transfer results that have been presented for the UHF case are rather limited in scope with regard to the ranges of buoyancy parameter Gr_x^*/Re_x^m and Prandtl numbers.

In the present paper, comprehensive results for the local and average Nusselt numbers are presented for the entire mixed convection regime, ranging from pure forced convection to pure free convection (i.e. for $0 \leqslant Gr_x^*/Re_x^m \leqslant \infty$), for a wide range of Prandtl numbers, $0.1 \leqslant Pr \leqslant 100$. The flow configurations covered include vertical, inclined and horizontal flat plates with uniform surface heat flux. Both buoyancy assisting and opposing flows are treated. The upper and lower bounds (a, b) of the significant mixed convection regime, $a \leqslant Gr_x/Re_x^m \leqslant b$, are established. In addition, simple correlation equations for the local and average Nusselt numbers are formulated for all the flow configurations. Such a comprehensive treatment of mixed convection flows on flat plates has not been carried out for the UHF case.

CORRELATIONS

The formulation and the treatment of laminar mixed convection flow adjacent to a semi-infinite flat plate with uniform heat flux, q_w, imposed on its surface have been presented for vertical, inclined and horizontal geometries [1]. That formulation was used to generate new numerical results for these flow configurations which cover the entire mixed convection regime for the buoyancy assisting and the buoyancy opposing flow conditions as shown in Figs. 1 and 2. These results were used to validate the accuracy of proposed simple correlations for the local and average mixed convection Nusselt numbers.